Genetic Modification of Bacillus subtilis for Production of D-chiro-Inositol, an Investigational Drug Candidate for Treatment of Type 2 Diabetes and Polycystic Ovary Syndrome

Yoshida, Ken-ichi ; Yamaguchi, Masanori ; Morinaga, Tetsuro ; Ikeuchi, Maya ; Kinehara, Masaki ; Ashida, Hitoshi

(Citation)
Applied and Environmental Microbiology,72(2):1310-1315

(Issue Date)
2006-02

(Resource Type)
journal article

(Version)
Version of Record

(URL)
https://hdl.handle.net/20.500.14094/90000254

APPLIED AND ENVIRONMENTAL MICROBIOLOGY, Feb. 2006, p. 1310–1315 Vol. 72, No. 2
0099-2240/06/$08.00+0 doi:10.1128/AEM.72.2.1310–1315.2006

Genetic Modification of *Bacillus subtilis* for Production of D-*chiro*-Inositol, an Investigational Drug Candidate for Treatment of Type 2 Diabetes and Polycystic Ovary Syndrome

Ken-ichi Yoshida,[1]* Masanori Yamaguchi,[2] Tetsuro Morinaga,[1] Maya Ikeuchi,[1] Masaki Kinehara,[1] and Hitoshi Ashida[1]

Department of Biofunctional Chemistry, Faculty of Agriculture, Kobe University, Kobe, Hyogo,[1] and Central Research Laboratories, Hokko Chemical Industry Co., Ltd., Atsugi, Kanagawa,[2] Japan

Received 14 September 2005/Accepted 21 November 2005

D-*chiro*-Inositol (DCI) is a drug candidate for the treatment of type 2 diabetes and polycystic ovary syndrome, since it improves the efficiency with which the body uses insulin and also promotes ovulation. Here, we report genetic modification of *Bacillus subtilis* for production of DCI from *myo*-inositol (MI). The *B. subtilis iolABC-DEFGHIJ* operon encodes enzymes for the multiple steps of the MI catabolic pathway. In the first and second steps, MI is converted to 2-keto-MI (2KMI) by IolG and then to 3D-(3,5/4)-trihydroxycyclohexane-1,2-dione by IolE. In this study, we identified *iolI* encoding inosose isomerase, which converts 2KMI to 1-keto-D-*chiro*-inositol (1KDCI), and found that IolG reduces 1KDCI to DCI. Inactivation of *iolE* in a mutant constitutively expressing the *iol* operon blocked the MI catabolic pathway to accumulate 2KMI, which was converted to DCI via the activity of IolI and IolG. The mutant was able to convert at least 6% of input MI in the culture medium to DCI.

Epimerization of the six hydroxyl-groups in inositol (1,2,3,4,5,6-cyclohexanehexol) results in the formation of up to nine stereoisomers, including *myo*-inositol (MI) and D-*chiro*-inositol (DCI) (Fig. 1, compounds 1 and 2). MI is widely distributed in nature and is available commercially, whereas DCI, the product of the epimerization of the C_1 hydroxyl group of MI, is relatively rare. Earlier reports noted the presence of minor amounts of DCI in animal and human tissue sources (13), and it has been shown that DCI and MI are identified as components of two different inositol phosphoglycan (IPG) molecules in mammalian systems (10, 11). The role of IPGs as putative insulin secondary messengers has been illustrated in numerous studies (3, 6, 7, 17). In response to insulin, IPGs are released from glycosylphosphatidylinositols in cell membranes. Following hydrolysis of membrane glycosylphosphatidylinositol by phospholipases, IPGs are released into the cytoplasm, where they affect some of the enzymes implicated in the activity of insulin. The insulin-mimetic effects of IPGs and their analogues have also been widely documented (7). DCI, as a component of IPGs, is more important than MI, since the IPGs functioning as the insulin mediators contain DCI exclusively (10). DCI is either absent or at a low concentration in urine and muscle biopsy mediator samples in patients with type 2 diabetes, compared with control subjects (9). Furthermore, a defect in in vivo DCI production was elucidated in insulin-sensitive tissue of type 2 diabetic rats showing insulin resistance (12). Thus, administered DCI could act to bypass the defective DCI production associated with insulin resistance and contribute to, at least, the partial restoration of insulin sensitivity and, subsequently, glucose disposal. In addition, although the mechanism has not been clarified, the administration of DCI to women with the polycystic ovary syndrome has been shown to reduce circulating insulin, decrease serum androgens, ameliorate some of the metabolic abnormalities (increased blood pressure and hypertriglyceridemia), and promote ovulation (5). Therefore, DCI is a promising investigational drug candidate for the treatment of type 2 diabetes and polycystic ovary syndrome.

In nature, DCI and its derivatives can be found chiefly in plants (2), fungi (16), and insects (4). In plants and insects, DCI is formed by an oxidoreductive epimerization of the C_1 hydroxyl of MI (4). A rich source of DCI is pinitol, a 3-*O*-methyl ether of DCI obtained from pinewood and legumes. Consequently, the hydrolysis of soybean-derived pinitol with concentrated hydrochloric acid has been proposed as a manufactured source of DCI. The fungus-derived antibiotic kasugamycin can be also used as a precursor for DCI (14). However, the chemical processes involved in the production of DCI from pinitol and kasugamycin are difficult to control and sometimes result in the formation of unwanted by-products. We have therefore designed a bioconversion process that facilitates the production of DCI from genetically manipulated *Bacillus subtilis*.

MATERIALS AND METHODS

Bacterial strains, plasmids, and growth conditions. *B. subtilis* 60015 (*trpC2 metC7*) is our standard laboratory strain. *B. subtilis* YF256 (*trpC2 metC7 iolE41 iolR*::*cat*) is a mutant derived from strain 60015, and its construction was described previously (23). YF256 was maintained on tryptose blood agar base (Difco) supplemented with 0.18% glucose. *Escherichia coli* strains JM109 (18)

* Corresponding author. Mailing address: Department of Biofunctional Chemistry, Faculty of Agriculture, Kobe University, 1-1 Rokkodai, Nada, Kobe, Hyogo 657-8501, Japan. Phone: 81-78-803-5862. Fax: 81-78-803-5815. E-mail: kenyoshi@kobe-u.ac.jp.

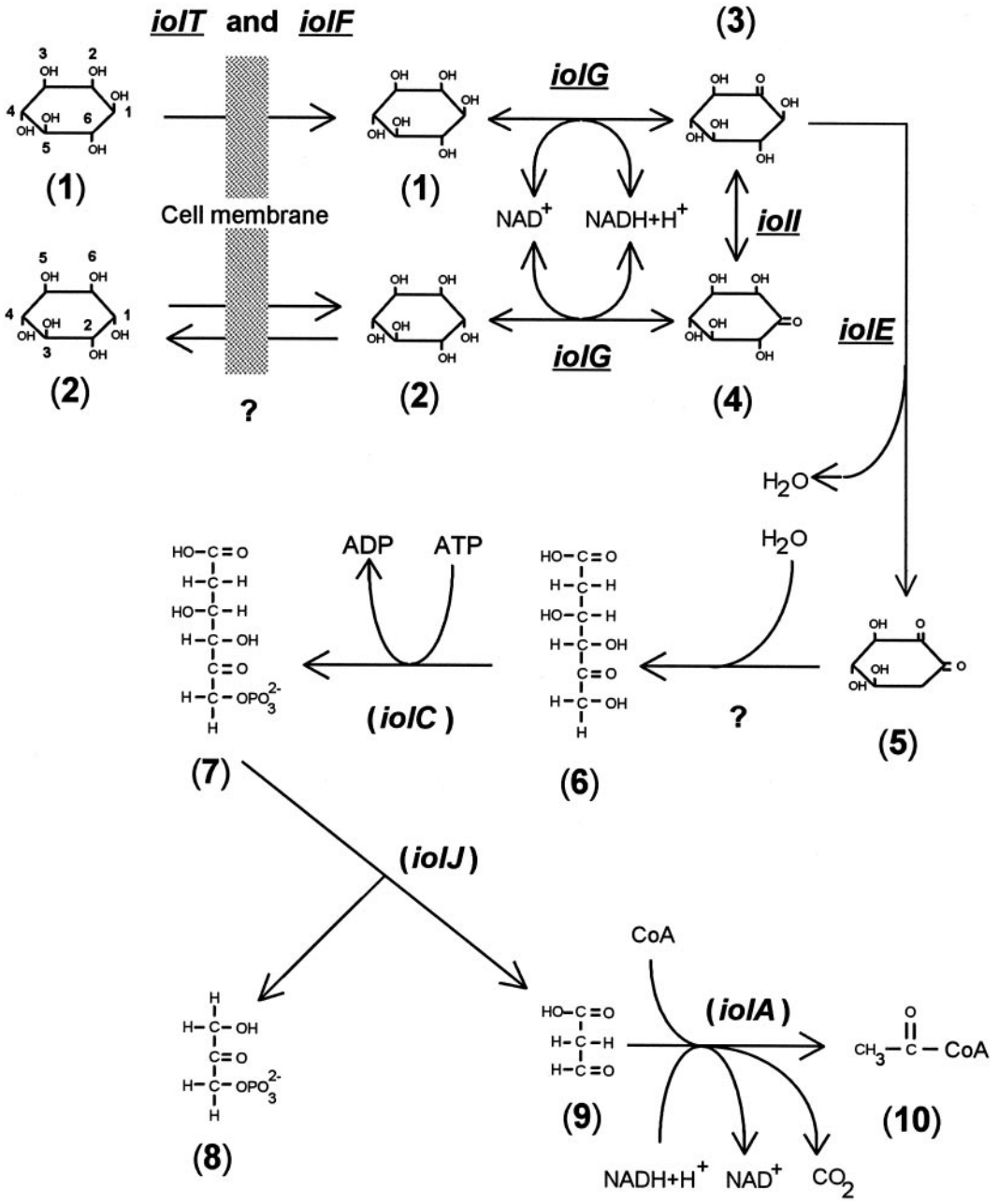

FIG. 1. MI catabolic pathway and functional activities of the *B. subtilis iol* genes. On the assumption that the pathway in *B. subtilis* is similar to that in *A. aerogenes* (1), *B. subtilis iol* genes proven and deduced (underlined and in parentheses, respectively) to encode the enzymes involved in the various reaction steps are shown (19, 22, 23), including the additional pathway involving IolI in the degradation of DCI. Compounds: 1, MI; 2, DCI (carbon numbering is indicated); 3, 2KMI; 4, 1KDCI; 5, 3D-(3,5/4)-trihydroxycyclohexane-1,2-dione; 6, 2-deoxy-5-keto-D-gluconic acid; 7, 2-deoxy-5-keto-D-gluconic acid 6-phosphate; 8, dihydroxyacetone phosphate; 9, malonic semialdehyde; 10, acetyl-coenzyme A.

and BL21(DE3) (Novagen) were used as the hosts for plasmid constructions and expression of the C-terminal His_6 tag fusion protein, respectively. *E. coli* strains were usually grown in Luria broth (15). Plasmids pET-30a(+) (Novagen) and pG-KJE8 (Takara) were used as cloning vectors for the His_6 tag fusion constructs and for supplying chaperones to stabilize overproduction of the fusion proteins, respectively. When required, media were supplemented with arabinose (1 mg/ml), chloramphenicol (15 and 35 μg/ml for *B. subtilis* and *E. coli*, respectively), isopropyl-β-D-thiogalactopyranoside (IPTG; 0.5 mM), kanamycin (50 μg/ml), and tetracycline (5 ng/ml).

Plasmid constructions. DNA fragments covering each of the *iolG* and *iolI* coding regions with flanking NdeI and XhoI sites at the proximal and distal ends, respectively, were amplified from DNA of strain 60015 by PCR using specific primer pairs; for *iolG*, iolGNdeI (5′-GGAATTCCATATGAGTTTACGTATTGGCGT-3′; the restriction site is underlined) and iolGXhoI (5′-CCGCTCGAGGTTTTGAACTGTTGTAAAAGA-3′) were used. For iolI, iolINdeI (5′-GGAATTCCATATGAAACTTTGTTTTAATGA-3′) and iolIXhoI (5′-CCGCTCGAGCATGCTGAAGTATTTTGATAC-3′) were used. Each of the fragments was trimmed with NdeI and XhoI and ligated with the NdeI-XhoI arm of

pET-30a(+). The ligated DNA was used for the transformation of *E. coli* strain JM109 to kanamycin resistance, resulting in plasmids pETiolG and pETiolI, which carried the respective *iol* genes with in-frame C-terminal fusion to a His_6 tag placed under the control of the pET-30a(+)-borne T7 promoter. Correct construction of each of the plasmids was confirmed by nucleotide sequencing.

Enzyme production and purification. pETiolG and pETiolI DNA was extracted from JM109 and introduced into strain BL21(DE3) together with pGKJE8. Strain BL21(DE3), carrying both plasmids, was inoculated into TGA medium (8) containing arabinose, chloramphenicol, kanamycin, and tetracycline and grown at 37°C with shaking. At an optical density at 600 nm of 0.35, production of the C-terminal His_6 tag fusion proteins was induced for 2 h by the addition of IPTG. The cells were harvested, treated with lysozyme, and disrupted by brief sonication; the soluble fraction was obtained after centrifugation. The His_6 tag fusion proteins were purified from the soluble fraction with the His-Bond system (Novagen), employing the standard procedure as recommended by the supplier. The purified proteins were subjected to Sephadex G-25 (Amersham) gel filtration to remove imidazol and salts. The purity of the His_6 tag fusion proteins was verified by sodium dodecyl sulfate-polyacrylamide gel electrophoresis and subsequent immunoblot analyses with anti-His tag antibody (Nacalai Tesque).

Enzyme reactions and detection of the reaction products. Reversible interconversion of 2-keto-MI (2KMI) and 1-keto-D-*chiro*-inositol (1KDCI) by IolI was analyzed as follows. Substrates (2KMI, 1KDCI, and 1-keto-L-*chiro*-inositol [1KLCI]) were supplied by Hokko Chemical Industry. The reaction mixture (100 μl) in 40 mM potassium phosphate buffer (pH 7.5) was composed of 88 μg of the purified His_6 tag fusion IolI enzyme, 1 mM $MnSO_4$, and 178 mM substrate (2KMI, 1KDCI, and 1KLCI). The mixture was incubated at 36°C for 120 min, and the reaction was terminated by the addition of DuoliteC20 (H^+ type) and incubation at 50°C at 10 min. After the addition of 200 μl of water, the supernatant was obtained by centrifugation; an aliquot (10 μl) was subjected to high-performance liquid chromatography (HPLC) analysis using a Wakosil5NH2 column (4.6 by 250 mm) kept at 20°C with a flow of acetonitrile/water (80/20) at 2 ml/min; signals for the compounds were detected by a refraction index sensor. Concentrations of the compounds were calculated from the peak area.

The reduction of 1KDCI to DCI, catalyzed by IolG, was examined as follows. A reaction mixture (200 μl) in 100 mM Tris-HCl (pH 8.5) was composed of 163 μg of the purified His_6 tag fusion IolG enzyme, 1 mM $MgSO_4$, 70 mM NADH, and 84 mM 1KDCI. The mixture was incubated at 36°C for 120 min. The reaction was terminated and subjected to HPLC analysis, as described above.

The IolI-IolG coupling reaction to convert MI to DCI was performed as follows. A reaction mixture (160 μl) in 50 mM Tris-HCl (pH 8.0) was composed of 177 μg of the purified His_6 tag fusion IolI enzyme, 65 μg of the purified His_6 tag fusion IolG enzyme, 1 mM $MgSO_4$, 0.1 mM $MnSO_4$, 0.5 mM NAD, 11 mM 2KMI, and 278 mM MI. The mixture was incubated at 36°C for 10 h. The reaction was terminated by being boiled for 10 min, and it was then diluted 10 times before being subjected to HPLC analysis as above.

Bioconversion of MI to DCI. For bioconversion of MI to DCI, a cell suspension of YF256 was inoculated, giving an initial optical density for the cells at 600 nm of 0.05, into a 500-ml Sakaguchi flask containing 30 ml of a broth medium consisting of 1% Bacto Soytone (Difco), 0.5% Bacto yeast extract (Difco), 0.5% NaCl, and 1% MI; it was then allowed to grow at 37°C with shaking at 150 rpm for 17 h (further cultivation led to almost no better yield of DCI under these conditions; data not shown). Cell growth (measured as an increase in optical density at 600 nm) was monitored, and the concentration of DCI appearing in the medium was determined by means of the HPLC analysis described above.

RESULTS AND DISCUSSION

Strains of *B. subtilis* possess an efficient MI catabolic pathway, encoded by the *iol* divergon (operons *iolABCDEFGHIJ* and *iolRS*) (19) and the *iolT* gene (22). A repressor, encoded by *iolR*, is responsible for the transcriptional regulation of the *iol* divergon and *iolT* (19, 22). In the absence of MI in the growth medium, the IolR repressor binds to the operator site within the promoter regions to repress transcription. However, in its presence, MI is converted to a catabolic intermediate that acts as an inducer, antagonizing IolR and leading to the induction of the *iol* divergon and *iolT* (20, 22). Thus, inactivation of *iolR* renders the transcription of the *iol* divergon and *iolT* constitutive (19).

The inositol catabolic pathway in *B. subtilis* has not been fully elucidated, but it is proposed to involve stepwise multiple reactions that ultimately yield dihydroxyacetone phosphate and acetyl-coenzyme A (Fig. 1, compounds 8 and 10). Inositol dehydrogenase, encoded by *iolG*, is responsible for the first step of the degradation cascade, producing 2KMI from MI (conversion of compound 1 to compound 3) (19). Inosose dehydratase, encoded by *iolE*, is responsible for the second step, producing 3D-(3,5/4)-trihydroxycyclohexane-1,2-dione (previously designated D-2,3-diketo-4-deoxy-*epi*-inositol) (compound 5) (23), while *iolT* and *iolF* encoded the primary and secondary inositol transporters, respectively (Fig. 1) (22). Based on the assumption that the catabolic pathway is the same as that proposed by Anderson and Magasanik for *Aerobacter aerogenes* (1), homology searches indicate that the products of the *iolC*, *iolJ*, and *iolA* genes are, respectively, likely to be responsible for the fourth, fifth, and sixth steps of the pathway (Fig. 1) (20).

iolI is the ninth gene of the *B. subtilis iol* operon, encoding a conserved 278-residue protein of unknown function. Its crystal structure is reported to have a beta-barrel (TIM) configuration, suggestive of structural homology to both endonuclease IV and xylose isomerase with a Zn^{2+}-binding fold (24). In this study, we found that *iolI* encoded an inosose isomerase functioning for the reversible interconversion of 2KMI and 1KDCI (Fig. 1, compound 4). *B. subtilis iolI* was expressed in *Escherichia coli* as a C-terminal His_6 tag fusion and purified. The purified enzyme was shown to interconvert 2KMI and 1KDCI (Fig. 2A), but it did not react with 1KLCI. The enzyme required metal ions such as Mn^{2+}, Fe^{2+}, or Co^{2+} for its activity, with a preference for Mn^{2+}, despite previous structural analysis demonstrating its capacity to bind Zn^{2+} (24). The enzyme showed a pH optimum of between pH 7.5 to 8.5. When the equilibrium of the forward and reverse reactions was established, it gave a mixture of 2KMI and 1KDCI at a molar ratio of 77:23 (Fig. 2A). On the other hand, inositol dehydrogenase encoded by *iolG*, which was also produced in *E. coli* and purified as a C-terminal His_6 tag fusion, was shown to be capable of reducing 1KDCI to DCI with oxidation of NADH (Fig. 2B). The IolG reaction to convert 1KDCI to DCI was also reversible, suggesting that *B. subtilis* could metabolize DCI, as well as MI. Indeed, we found that *B. subtilis* 60015 was able to utilize DCI as a sole carbon source (data not shown).

The IolI and IolG reactions were coupled in vitro to show conversion of MI to DCI (Fig. 2C), and the overall equilibrium of the forward and reverse reactions gave a mixture of DCI and MI at a ratio of 14:86. These results raised the possibility of genetically manipulating *B. subtilis* to produce DCI from MI. To investigate this possibility, cells of *B. subtilis* strain YF256 (*iolE41*), which are not able to utilize MI as the sole carbon source due to a defect in IolE (23), were grown in a broth medium containing 1% MI (Fig. 3). The *iolE41* mutation prevents the production of the intermediate that antagonizes IolR (23) which, together with an *iolR*::*cat* mutation, allows constitutive expression of the entire *iol* operon (19) containing *iolG* and *iolI*, as well as *iolT* (22). Therefore, cells of this strain take up MI efficiently and accumulate 2KMI because of a blockage at the second step in the MI catabolism pathway catalyzed by IolE. Subsequently, it was expected that the accumulated 2KMI would provide a substrate for the IolI/IolG coupling

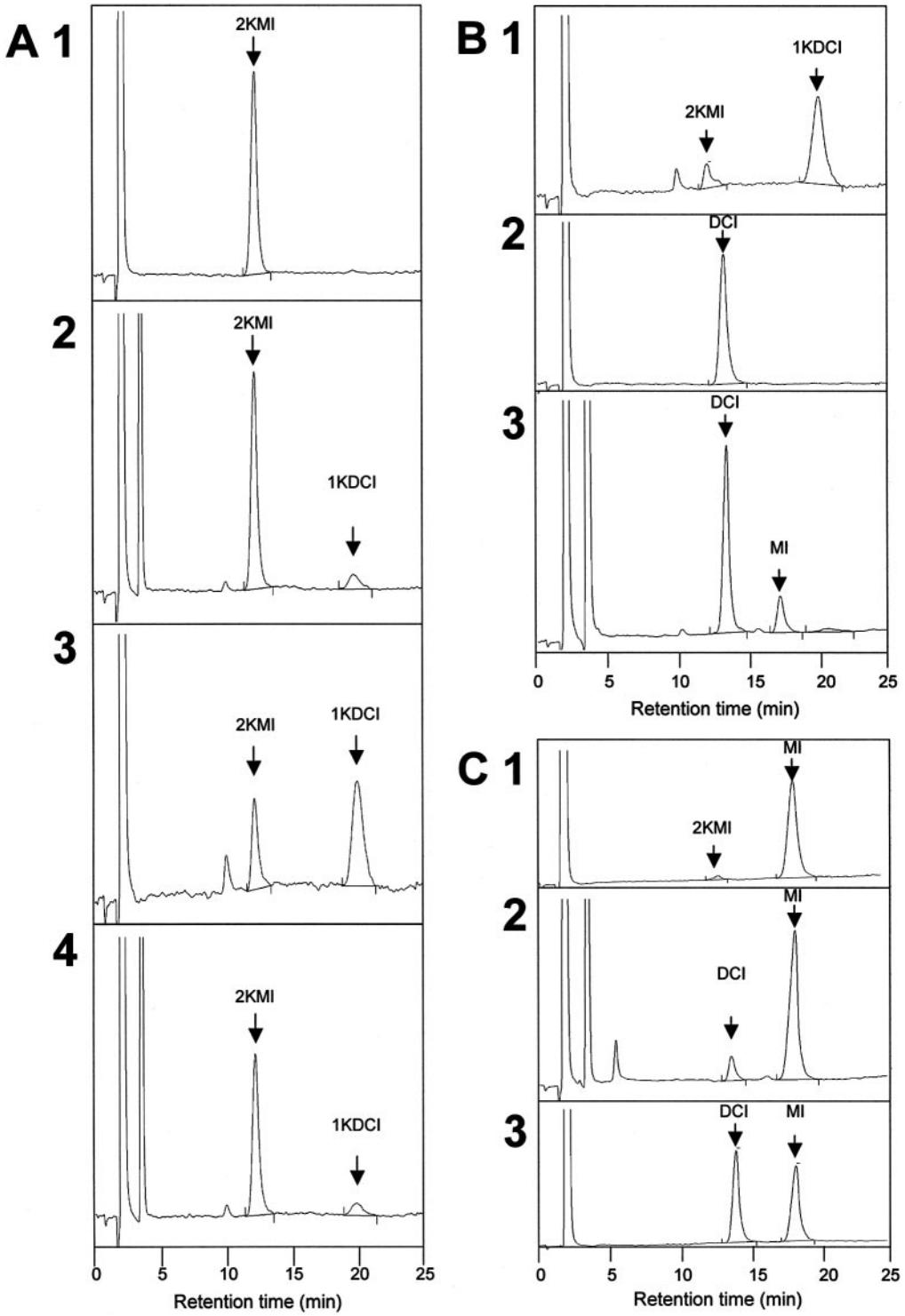

FIG. 2. HPLC analysis of the products of IolI and IolG reactions. The reactions were carried out as described in the text. (A) Forward and reverse reactions catalyzed by inosose isomerase encoded by *iolI*. Four HPLC charts analyzing the substrates and products are shown: 1, 2KMI standard (substrate before the forward reaction); 2, after the forward reaction; 3, 1KDCI standard (substrate before the reverse reaction), containing 2KMI from the beginning; 4, after the reverse reaction. Peaks for 2KMI and 1KDCI are indicated. Note that charts 2 and 4 are almost identical, suggesting establishment of equilibrium of the forward and reverse reactions. Minor peaks at 10 min are probably due to (±)-2-keto-*epi*-inositol derived from spontaneous isomerization of 1KDCI. Glycerol contained in the enzyme solution gave the high peaks at around 3 min. (B) Reduction of 1KDCI to DCI by inositol dehydrogenase encoded by *iolG*. Three HPLC charts analyzing the substrates and products are shown: 1, 1KDCI standard (substrate before the reaction); 2, DCI standard; 3, after the reaction (MI was produced by reduction of 2KMI contained in the 1KDCI sample). Peaks for 1KDCI, 2KMI, MI, and DCI are indicated. (C) IolI/IolG coupling reaction to convert MI to DCI. Three HPLC charts are shown: 1, before the coupling reaction; 2, after the reaction; 3, MI and DCI standards. Peaks for MI, 2KMI, and DCI are indicated.

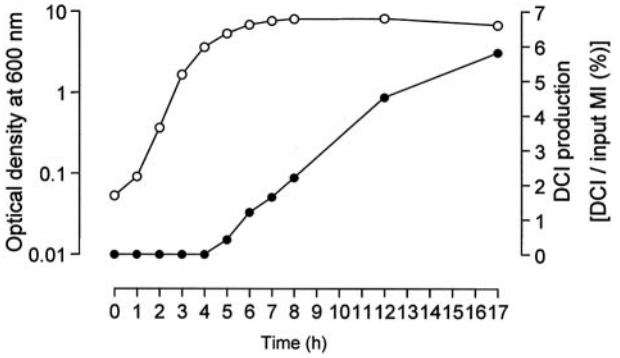

FIG. 3. Bioconversion of MI to DCI. *B. subtilis* YF256 was grown in a broth medium containing 1% MI, as described in the text. Cell growth (increase in optical density at 600 nm) (open circles) was monitored throughout growth. The concentration of DCI in the medium was determined by means of the HPLC analysis (Fig. 2) and presented as the percentages of the input MI (solid circles). Representative data from three independent experiments are shown.

reaction to be converted to DCI. As shown (Fig. 3), the accumulation of DCI in the growth medium during transition from logarithmic growth to stationary phase and during the latter confirmed the formation of DCI by this strain; the highest yield of DCI under the conditions we used was 6% of the input MI. Before and after the bioconversion, the total amounts of MI and DCI were constant, suggesting that the input MI was not being used as a carbon source for growth but exclusively for conversion to DCI. After polar substances contained in the culture medium were removed, the synthesized DCI and remaining MI could be separated and purified by conventional chromatography, the MI being recycled for subsequent bioconversion. These results suggest that bioconversion of MI to DCI by genetically manipulated *B. subtilis* provides a novel and simple method for producing DCI.

Since transcription of the *iol* operon and *iolT* in the mutant is driven constitutively because of the inactivation of *iolR* (19, 22), the conversion of MI to DCI might be expected to take place during exponential growth. However, no DCI appeared in the growth medium before the transition phase (Fig. 3). This observation suggested that expression of the *iol* genes and/or enzyme activity of their products involved in the interconversion of MI and DCI might not be sufficient during exponential growth. Previous studies demonstrated that activity of inositol dehydrogenase encoded by *iolG* in an *iolR* mutant was still under partial catabolite repression by a mechanism that is independent of the major glucose repression mediated by CcpA (19, 21). Furthermore, the efficiency in bioconversion of MI to DCI can vary widely, depending on the composition of the medium (data not shown). Therefore, it is conceivable that during exponential growth the better nutritional conditions could render expression of the *iol* genes and/or enzyme activity insufficient through unidentified repression mechanisms.

The yield of DCI following the bioconversion is, at 6%, approximately 43% of the yield (14%) expected from the in vitro interconversion of MI and DCI discussed above (Fig. 2C). Currently, we do not know what is limiting this interconversion in vivo, which might involve either feedback inhibition or membrane transport. In the latter case, we do not know if there is a specific transport system for the export of DCI into the medium. If a specific exporter could be identified, it would provide a good candidate to be reinforced to improve the yield. Another possible reason for the lower yield might be the reduced concentration of NADH during the bioconversion, since NADH produced by the conversion of MI to 2KMI could be required not only for reduction of 1KDCI to DCI, but also for energy production via the respiration chain. Therefore, higher DCI yields might be achieved by the provision of alternative substrates for the enrichment of the NADH pool during the bioconversion.

ACKNOWLEDGMENTS

We thank Y. Tanaka for his technical assistance and C. R. Harwood for his critical reading of the manuscript and valuable suggestions.

REFERENCES

1. **Anderson, W. A., and B. Magasanik.** 1971. The pathway of *myo*-inositol degradation in *Aerobacter aerogenes*. Conversion of 2-deoxy-5-keto-D-gluconic acid to glycolytic intermediates. J. Biol. Chem. **246:**5662–5675.
2. **Drew, E. A.** 1983. Physiology and biochemistry of storage carbohydrates in vascular plants. Cambridge University Press, Cambridge, United Kingdom.
3. **Field, M. C.** 1997. Is there evidence for phospho-oligosaccharides as insulin mediators? Glycobiology **7:**161–168.
4. **Hipps, P. P., R. K. Sehgal, W. H. Holland, and W. R. Sherman.** 1973. Identification and partial characterization of inositol: NAD^+ epimerase and inosose: NAD(P)H reductase from the fat body of the American cockroach, Periplaneta americana L. Biochemistry **12:**4705–4712.
5. **Iuorno, M. J., D. J. Jakubowicz, J. P. Baillargeon, P. Dillon, R. D. Gunn, G. Allan, and J. E. Nestler.** 2002. Effects of D-*chiro*-inositol in lean women with the polycystic ovary syndrome. Endocr. Pract. **8:**417–423.
6. **Jones, D. R., and I. Varela-Nieto.** 1998. The role of glycosyl-phosphatidylinositol in signal transduction. Int. J. Biochem. Cell Biol. **30:**313–326.
7. **Jones, D. R., and I. Varela-Nieto.** 1999. Diabetes and the role of inositol-containing lipids in insulin signaling. Mol. Med. **5:**505–514.
8. **Kaempfer, R. O., and B. Magasanik.** 1967. Effect of infection with T-even phage on the inducible synthesis of beta-galactosidase in *Escherichia coli*. J. Mol. Biol. **27:**453–468.
9. **Kennington, A. S., C. R. Hill, J. Craig, C. Bogardus, I. Raz, H. K. Ortmeyer, B. C. Hansen, G. Romero, and J. Larner.** 1990. Low urinary *chiro*-inositol excretion in non-insulin-dependent diabetes mellitus. N. Engl. J. Med. **323:**373–378.
10. **Larner, J., L. C. Huang, C. F. Schwartz, A. S. Oswald, T. Y. Shen, M. Kinter, G. Z. Tang, K. Zeller.** 1988. Rat liver insulin mediator which stimulates pyruvate dehydrogenase phosphatase contains galactosamine and D-*chiro*-inositol. Biochem. Biophys. Res. Commun. **151:**1416–1426.
11. **Larner, J., L. C. Huang, S. Suzuki, G. Tang, C. Zhang, C. F. Schwartz, G. Romero, L. Luttrell, and A. S. Kennington.** 1989. Insulin mediators and the control of pyruvate dehydrogenase complex. Ann. N. Y. Acad. Sci. **573:**297–305.
12. **Larner, J.** 2002. D-*chiro*-inositol—its functional role in insulin action and its deficit in insulin resistance. Int. J. Exp. Diabetes. Res. **3:**47–60.
13. **Niwa, T., N. Yamamoto, K. Maeda, and K. Yamada.** 1983. Gas chromatographic-mass spectrometric analysis of polyols in urine and serum of uremic patients. Identification of new deoxyalditols and inositol isomers. J. Chromatogr. **277:**25–39.
14. **Pak, Y., L. C. Huang, K. J. Lilley, and J. Larner.** 1992. *In vivo* conversion of [^{3}H]myoinositol to [^{3}H]chiroinositol in rat tissues. J. Biol. Chem. **267:**16904–16910.
15. **Sambrook, J., and D. W. Russell.** 2001. Molecular cloning: a laboratory manual, 3rd ed. Cold Spring Harbor Laboratory Press, Cold Spring Harbor, N.Y.
16. **Umezawa, H., M. Hamada, Y. Suhara, T. Hashimoto, and T. Ikekawa.** 1965. Kasugamycin, a new antibiotic. Antimicrob. Agents Chemother. **5:**753–757.
17. **Varela-Nieto, I., Y. Leon, and H. N. Caro.** 1996. Cell signaling by inositol phosphoglycans from different species. Comp. Biochem. Physiol. **115:**223–241.
18. **Yanisch-Perron, C., J. Vieira, and J. Messing.** 1985. Improved M13 phage cloning vectors and host strain: nucleotide sequences of M13mp18 and pUC19 vectors. Gene **33:**103–119.
19. **Yoshida, K., D. Aoyama, I. Ishio, T. Shibayama, and Y. Fujita.** 1997. Organization and transcription of the *myo*-inositol operon, *iol*, of *Bacillus subtilis*. J. Bacteriol. **179:**4591–4598.
20. **Yoshida, K., T. Shibayama, T., D. Aoyama, and Y. Fujita.** 1999. Interaction of a repressor and its binding sites for regulation of the *Bacillus subtilis iol* divergon. J. Mol. Biol. **285:**917–929.
21. **Yoshida, K., K. Kobayashi, Y. Miwa, C.-M. Kang, M. Matsunaga, H.**

Yamaguchi, S. Tojo, M. Yamamoto, R. Nishi, N. Ogasawara, T. Nakayama, and Y. Fujita. 2001. Combined transcriptome and proteome analysis as a powerful approach to study genes under glucose repression in *Bacillus subtilis*. Nucleic Acids Res. **29:**683–692.

22. **Yoshida, K., Y. Yamamoto, K. Omae, M. Yamamoto, and Y. Fujita.** 2002. Identification of two *myo*-inositol transporter genes of *Bacillus subtilis*. J. Bacteriol. **184:**983–991.
23. **Yoshida, K., M. Yamaguchi, H. Ikeda, K. Omae, K. Tsurusaki, and Y. Fujita.** 2004. The fifth gene of the *iol* operon of *Bacillus subtilis*, *iolE*, encodes 2-keto-*myo*-inositol dehydratase. Microbiology **150:**571–580.
24. **Zhang, R. G., I. Dementieva, N. Duke, F. Collart, E. Quaite-Randall, R. Alkire, L. Dieckman, N. Maltsev, O. Korolev, and A. Joachimiak.** 2002. Crystal structure of *Bacillus subtilis* IolI shows endonuclease IV fold with altered Zn binding. Proteins **48:**423–426.